

# Internal conversion of the low energy $^{229m}\text{Th}$ isomer in the Thorium anion

E. V. Tkalya<sup>1,2,3,\*</sup> and R. Si<sup>4,5</sup>

<sup>1</sup>*P.N. Lebedev Physical Institute of the Russian Academy of Sciences, 119991, 53 Leninskiy pr., Moscow, Russia*

<sup>2</sup>*National Research Nuclear University MEPhI, 115409, Kashirskoe shosse 31, Moscow, Russia*

<sup>3</sup>*Nuclear Safety Institute of RAS, Bol'shaya Tuskaya 52, Moscow 115191, Russia*

<sup>4</sup>*Shanghai EBIT Lab, Key Laboratory of Nuclear Physics and Ion-beam Application, Institute of Modern Physics, Department of Nuclear Science and Technology, Fudan University, Shanghai 200433, Peoples Republic of China*

<sup>5</sup>*Spectroscopy, Quantum Chemistry and Atmospheric Remote Sensing (SQUARES), CP160/09, Universit'e libre de Bruxelles, Av. F.D. Roosevelt 50, 1050 Brussels, Belgium*

(Dated: April 30, 2020)

A process of the decay of the anomalously low lying nuclear isomer  $^{229m}\text{Th}(3/2^+, 8.28 \pm 0.17 \text{ eV})$  in the Thorium anion ( $\text{Th}^-$ ) via the internal conversion (IC) channel is studied. We show that the half life of the nuclear isomer in the  $6d_{3/2}^3 7s_{1/2}^2$  ground state and in the  $6d_{3/2}^2 7s_{1/2}^2 7p_{1/2}^1$  excited state of  $\text{Th}^-$  is  $\approx 1.5$  and  $\approx 1.1$  times bigger than in the  $6d_{3/2}^2 7s_{1/2}^2$  ground state of the Th atom. The IC probabilities in the anion decreases despite the decay via the additional  $6d_{3/2}$  or  $7p_{1/2}$  electrons. This counterintuitive result is a consequence: a) of a decrease in the amplitudes of the  $6d_{3/2}$  and  $7s_{1/2}$  wave functions near the nucleus due to an increase in their diffuseness of upon the addition of extra electron, b) of mutual compensation in the IC probability due to a kinematic factor, which depends on the energy of the conversion electron in the continuum as  $E_c^{-1/2}$ , and the  $E_c^{1/4}$  growth of the amplitudes of the electron wave functions.

PACS numbers: 23.20.Nx, 21.10.Tg, 27.90.+b

## I. INTRODUCTION

The  $^{229}\text{Th}$  nucleus has a unique low-lying isomeric state  $^{229m}\text{Th}(3/2^+, E_{\text{is}} = 8.28 \pm 0.17 \text{ eV})$  [1]. The dramatic and controversial story of the experimental studies of this state — the discovering of the level [2–12], the measuring its energy [1–3, 13–17], magnetic and quadrupole moments [18], charge radius [19], and half-life [15, 16] is still far from complete. Increasing the accuracy of the measurements is important for the creation of ultra precise clock at the nuclear transition of the optical range [20–23], which in turn can be used to study the relative effects of the variation of the fine structure constant and the strong interaction parameter [24–26]. Investigations of this nuclear state are important for the design the laser at the nuclear transition [27, 28], to control the isomeric level  $\gamma$  decay via boundary conditions [29], to detect the decay of the ground state sublevel of the nucleus into the isomeric state sublevel in the muonic atom  $^{229}\text{Th}$  [30], to check the exponentiality of the decay law of at long times [31] and others.

We know now five possible decay channels of the  $^{229m}\text{Th}$  isomer — four processes where the electron shell is involved, and the alpha decay. It is natural to systematize the first four channels in the framework of the perturbation theory for the quantum electrodynamics using the order of relevant Feynman diagrams [32].

In the first order of the perturbation theory, this is the process of the emission of a photon by the nucleus, which

for low-energy nuclear levels is practically unobservable. However, the photon observation is possible if the  $^{229m}\text{Th}$  isomer is put in the dielectrics with a large band gap, where the thorium atom becomes effectively “ionized” by the chemical environment. For the first time, this possibility was indicated in [33, 34].

Internal conversion (IC) is a second-order process. IC is the main decay channel of the isomer  $^{229m}\text{Th}$  on the valence shells of the ground state of the Th atom [35], on the excited atomic states of Th [35, 36], and on the Rydberg states [37]. Experimentally, IC was observed in Refs. [15, 16, 38]. Another second-order process, namely, the decay of the  $^{229m}\text{Th}$  isomer during inelastic scattering by metal conduction electrons, was considered in [8]. The nuclear excitation by electron transition (NEET) [39] is also of the second order process. A detailed theory of NEET is given in [40, 41]. This process can play an important role as an integral part of the electron bridge.

Electron bridge, a third-order process suggested in [42], was considered for the decay and excitation of  $^{229m}\text{Th}$  in Refs. [35, 43, 44]. Later, this process was thoroughly studied theoretically (see in [45–51]), and there are high hopes for the effective excitation of the  $^{229}\text{Th}$  nuclei in ion traps.

The  $\alpha$  decay of  $^{229m}\text{Th}$  considered in [52, 53] is an important decay channel. The detection of this process or accompanying bremsstrahlung [54] could be the most reliable proof of both the existence of the  $^{229m}\text{Th}$  isomer and its excitation by the laser radiation [46].

In this paper, we investigate the decay of  $^{229m}\text{Th}$  in the thorium anion,  $\text{Th}^-$ . Anions are negative ions created when an atom gains one or more electrons. Particularly often the anions are formed from the chemical elements

---

\*Electronic address: tkalya'e@lebedev.ru

in the groups 17 and 16 of the Periodic table ( $F^-$ ,  $O^{2-}$  and so on). These elements lack, respectively, one or two electrons with respect to the complete electronic configuration of a noble gas. However, anions of the other chemical elements can be formed in various physicochemical processes, too. Laser plasma is a well-studied universal source of the negative ions [55]. The laser ablation method allows one to get the anions of any chemical element in the Periodic table. In the laser plasma, anions are produced at a certain stage of the expansion during cooling of the plasma bunch after the end of the laser pulse. Typical values of the negative ion currents are tens to hundreds of microamperes. In Ref. [56], the  $Th^-$  anions were produced via the pulsed Nd:Y-Al-garnet laser ablation of a thorium metal disk. Further, the anions were accumulated and cooled via buffer gas cooling in the ion trap. After that, anions were photodetached by a tunable dye laser and the outgoing photoelectrons were detected.

It turned out that  $Th^-$  is a stable system with the ionization potential of about 0.6 eV [56, 57]. It has at least a couple of levels connected by a strong electric dipole transition suitable for laser cooling [56]. Since the cooled ions in traps manipulated by laser and the laser ablation (which produces plasma contained as well as positive and negatively charged ions), as a method of loading the ion trap, are currently considered as a promising system for studying of  $^{229m}Th$ , the knowledge of the decay channels and the lifetime of the  $^{229m}Th$  isomer in anions can be very useful for future experimental research.

## II. INTERNAL CONVERSION IN $Th^-$

Until recently, the  $6d_{3/2}^2 7s_{1/2}^2 7p_{1/2}^1 \ ^4G_{5/2}^o$  state with the binding energy of 0.368 eV was considered as the ground state of the thorium anion [57]. However, as has been shown in [56],  $6d_{3/2}^2 7s_{1/2}^2 7p_{1/2}^1 \ ^4G_{5/2}^o$  is an excited state, and the true ground state of  $Th^-$  is the configuration  $6d_{3/2}^3 7s_{1/2}^2 \ ^4F_{3/2}$  with the binding energy of 0.6 eV. In addition, there are several strong electric dipole transitions between the bound levels arising from configurations  $6d_{3/2}^3 7s_{1/2}^2$  and  $6d_{3/2}^2 7s_{1/2}^2 7p_{1/2}^1$ . These conclusions have been reached on the basis of measurements of the ionization potential for the Thorium anion, and large-scale numerical multiconfiguration Dirac-Hartree-Fock calculations [56, 58].

In the following, we present the analysis of the internal conversion, which uses the bound state wave functions obtained in Ref. [56]: the  $6d_{3/2}^2 7s_{1/2}^2$  wave function for the ground state of the Thorium atom ( $Th$ ), the  $6d_{3/2}^2 7s_{1/2}^2$  wave function for the ground state of the anion ( $Th^-$ ), and the  $6d_{3/2}^2 7s_{1/2}^2 7p_{1/2}^1$  wave function for the anion excited state ( $Th^{*-}$ ). Thus, we are able to compare the internal conversion coefficients (ICC) for the  $Th$  atom and anions, obtained within the same approach. This is important because different codes can give significantly

different results when one calculates ICC from valence shells at ultra-low energy nuclear transition (see below Table IV).

The internal conversion coefficients per one electron for the  $E(M)L$  nuclear transition with the energy  $\omega_N = E_{is}$  were calculated using the formulas

$$\alpha_{E/ML} = \frac{\omega_N}{m} \frac{E+m}{p} \frac{L}{L+1} \sum_f \left( C_{j_i 1/2 L 0}^{j_f 1/2} \right)^2 |\mathcal{M}_{if}^{E/ML}|^2, \quad (1)$$

where  $m$  is the mass of the electron,  $E$  and  $p$  are the energy and momentum of the conversion electron satisfying the condition  $E^2 = m^2 + p^2$  (the system of units is  $\hbar = c = 1$ ),  $j$  is the total angular momentum of the electron,  $C_{j_i 1/2 L 0}^{j_f 1/2}$  is the Clebsch-Gordan coefficient. The electron matrix elements in Eq. (1) are

$$\begin{aligned} \mathcal{M}_{if}^{EL} &= \int_0^\infty h_L^{(1)}(\omega_N a_B x) [g_i(x)g_f(x) + f_i(x)f_f(x)] x^2 dx, \\ \mathcal{M}_{if}^{ML} &= \frac{\kappa_i + \kappa_f}{L} \int_0^\infty h_L^{(1)}(\omega_N a_B x) [g_i(x)f_f(x) + \\ &\quad f_i(x)g_f(x)] x^2 dx. \end{aligned} \quad (2)$$

Here  $x = r/a_B$ ,  $a_B$  is the Bohr radius,  $h_L^{(1)}(\omega_N a_B x)$  is the Hankel function of the first kind [59],  $\kappa = l(l+1) - j(j+1) - 1/4$ , where  $l$  is the orbital angular momentum of the electron.

One can use the well-known representation for the Clebsch-Gordan coefficient through the  $6j$  symbol [60]

$$\left( C_{j_i 1/2 L 0}^{j_f 1/2} \right)^2 = (2l_i + 1)(2j_f + 1) \left( C_{l_i 0 L 0}^{l_f 0} \right)^2 \left\{ \begin{matrix} l_i & 1/2 & j_i \\ j_f & L & l_f \end{matrix} \right\}^2 \quad (3)$$

in order for the selection rules for the parity and the orbital angular momentum in Eq. (1) to be satisfied automatically. In this case, the  $l_i \rightarrow l'_i = 2j_i - l_i$  substitution should be made in Eq. (3) for the magnetic type nuclear transitions.

In the case we are considering here, the nuclear transition energy is small and the following conditions are fulfilled:  $E_b < \omega_N \ll 1/a_B$ , where  $E_b$  is the electron binding energy in the initial state. Therefore, Eqs. (1–2) take the form

$$\begin{aligned} \alpha_{E/ML} &= e^2 \sqrt{\frac{2m}{\omega_N - E_b}} \frac{[(2L-1)!!]^2}{(\omega_N a_B)^{2L+1}} \frac{L}{L+1} \\ &\quad \sum_f \left( C_{j_i 1/2 L 0}^{j_f 1/2} \right)^2 |m_{if}^{E/ML}|^2, \end{aligned} \quad (4)$$

where the new electron matrix elements are

$$\begin{aligned} m_{if}^{EL} &= \int_0^\infty [g_i(x)g_f(x) + f_i(x)f_f(x)] x^{2-L-1} dx, \\ m_{if}^{ML} &= \frac{\kappa_i + \kappa_f}{L} \int_0^\infty [g_i(x)f_f(x) + f_i(x)g_f(x)] x^{2-L-1} dx. \end{aligned} \quad (5)$$

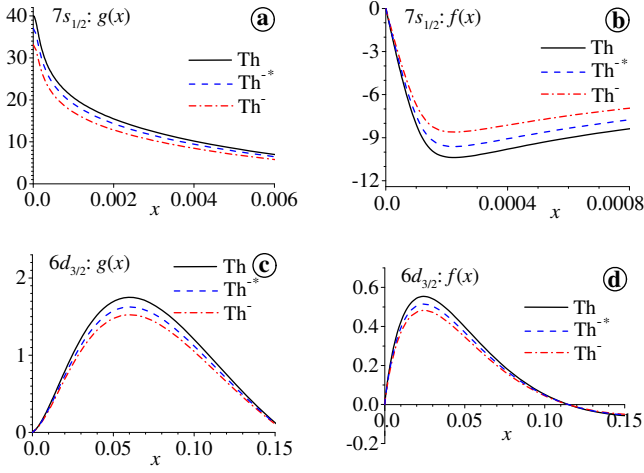


Figure 1: Wave functions of the  $7s_{1/2}$  and  $6d_{3/2}$  electron states in the Th atom and Thorium anion in the ground and excited states: (a) and (c) — the large  $g_i(x)$  components, (b) and (d) — the small  $f_i(x)$  components of the Dirac bispinor.

The energy of the nonrelativistic conversion electron in the continuum is  $E_c = mv^2/2 = \omega_N - E_b$ , where  $v$  is the electron speed. Thus, the factor  $\sqrt{2m/(\omega_N - E_b)}$  in Eq. 4 is equal to  $2/v$ . We will see below that this factor significantly “increases” the internal conversion coefficient in the Th atom (whose valence shells have a binding energy of about 6–7 eV), because it compensates for the small amplitudes of the electronic wave functions in the continuum.

The matrix elements (2) and (5) were calculated by numerical integration. We used the wave functions from the work [56] for the initial states, and the wave functions of the continuum for the final state.

The wave functions of the initial state are shown partly in Fig. 1 (these regions give main contributions to the electronic matrix elements). Extra electron contributes to an additional nuclear screening for other valence electrons. As a result, the electron shell becomes more diffuse. This is clearly seen in Fig. 2 — the average orbital radius of the  $6d_{3/2}$  and  $7s_{1/2}$  states increases when an electron is added to the  $7p_{1/2}$  and  $6d_{3/2}$  states of the Thorium atom. (Note also, in the  $6d_{3/2}^2 7s_{1/2}^2 7p_{1/2}^1$  anion excited state, the average radii  $\langle 6d_{3/2}|x|6d_{3/2}\rangle$  and  $\langle 7s_{1/2}|x|7s_{1/2}\rangle$  are smaller than the corresponding radii in the  $6d_{3/2}^3 7s_{1/2}^2$  ground state. It can be easily explained — the  $7p_{1/2}$  shell shields the nuclear charge less effectively than the  $6d_{3/2}$  shell because  $\langle 7p_{1/2}|x|7p_{1/2}\rangle > \langle 6d_{3/2}|x|6d_{3/2}\rangle$ , Fig. 2.)

As a result of the indicated “swelling”, on the one hand, and the conservation of the normalization volume of the wave functions, on the other hand, the amplitudes of the  $7s_{1/2}$  and  $6d_{3/2}$  wave functions decrease in the region near the nucleus, Fig. 1.

The wave functions of the continuum spectrum are the numerical solutions of the Dirac equations with the elec-

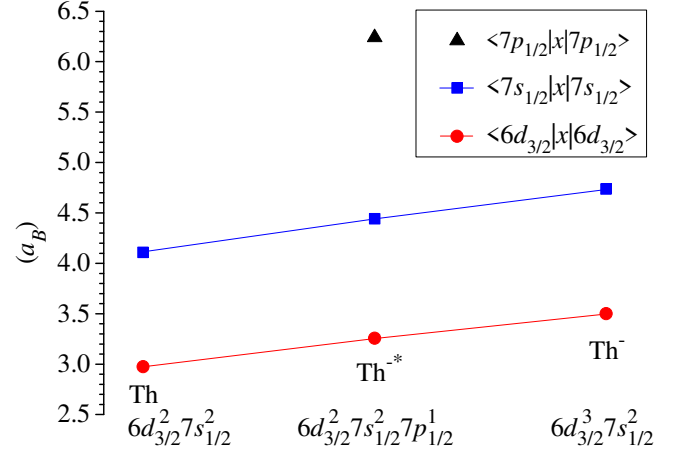


Figure 2: Averaged radii of the  $7p_{1/2}$ ,  $7s_{1/2}$  and  $6d_{3/2}$  orbitals in various electron configurations.

tron energies  $E > m$  ( $E \approx E_c + m$ )

$$\begin{aligned} g'(x) + \frac{1+\kappa}{x}g(x) - \frac{1}{e^2} \left( \frac{E}{m} + 1 - \frac{V(x)}{m} \right) f(x) &= 0, \\ f'(x) + \frac{1-\kappa}{x}f(x) + \frac{1}{e^2} \left( \frac{E}{m} - 1 - \frac{V(x)}{m} \right) g(x) &= 0, \end{aligned} \quad (6)$$

normalized at  $x \rightarrow \infty$  with the condition  $g_f(x) = \sin(pa_B x + \varphi_{ij})/x$ , where  $\varphi_{ij}$  is a phase. In Eq. (6),  $e$  is the electron charge.

As an example, two wave functions of the final state are shown in Fig. 3 for the IC transitions  $7s_{1/2} \rightarrow S_{1/2}$  and  $6d_{3/2} \rightarrow D_{1/2}$ . The energies of conversion electrons are:  $E_c(S_{1/2}) = 1.79$  eV and  $E_c(D_{3/2}) = 1.03$  eV for IC in the Th atom,  $E_c(S_{1/2}) = 6.68$  eV and  $E_c(D_{3/2}) = 7.65$  eV for IC in the Th anion in the ground state, and  $E_c(S_{1/2}) = 5.63$  eV and  $E_c(D_{3/2}) = 5.47$  eV for IC in the Th anion in the excited state. The solutions  $g_f(x)$  (and  $f_f(x)$ ) of Eq. (6) reliably reach the asymptotic behavior  $xg_f(x) = \text{Const} \times \sin(pa_B x)$  at  $x \approx 300$  in the Th<sup>+</sup> potential (for IC in the Th atom) and at  $x \approx 30$  in the potential of the Th atom (for IC in Th<sup>-</sup> and Th<sup>-\*</sup>). Further, the obtained wave functions  $g_f(x)$  and  $f_f(x)$  are renormalized by dividing by the constant “Const”.

The potential energy  $V(x)$  of the electron in Eq. 6 is  $V(x) = V_{\text{nucl}}(x) + V_{\text{shell}}(x)$ , where  $V_{\text{shell}}(x)$  is the potential energy of the electron in the shell electron potential, and  $V_{\text{nucl}}(x)$  is the potential energy of electron in potential of the unscreened nucleus. That is, the positive charge,  $Z$ , has been uniformly distributed within a sphere of the radius  $x_{R_0} = R_0/a_B$  ( $R_0 = 1.2A^{1/3}$  fm is the radius of the nucleus with the atomic number  $A$ ):  $V_{\text{nucl}}(x) = -\mathcal{E}_0(Z/2x_{R_0})[3 - (x/x_{R_0})^2]$  for  $0 \leq x \leq x_{R_0}$ , and  $V_{\text{nucl}}(x) = -\mathcal{E}_0 Z/x$  for  $x \geq x_{R_0}$  where  $\mathcal{E}_0 = me^4$  is the atomic unit of energy.

The electron shell potential has been found by solving the Poisson equation with the given electron density. The electron density in the Th<sup>+</sup> ion and in the Th atom for the IC calculations in the Th atom and in the Th<sup>-</sup> anion

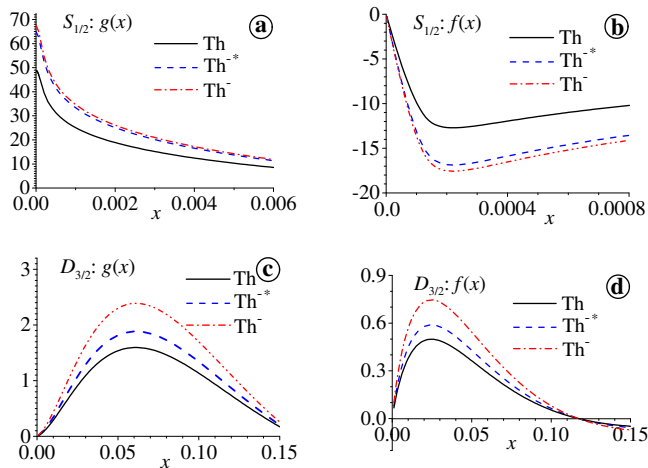


Figure 3: Wave functions of the  $S_{1/2}$  and  $D_{3/2}$  electron states in the continuum after IC on the  $7s_{1/2}$  and  $6d_{3/2}$  electron states in Th,  $\text{Th}^-$  and  $\text{Th}^{-*}$ : (a) and (c) — the large  $g_f(x)$  components, (b) and (d) — the small  $f_f(x)$  components of the Dirac bispinor.

respectively has been obtained within the DFT theory [61, 62] through the self-consistent procedure taking into account the exchange and correlation effects. Moreover, for the internal conversion in the neutral Th atom we consider two various electron densities for  $\text{Th}^+$ , corresponding to the  $6d_{3/2}^2 7s_{1/2}^1$  and  $6d_{3/2}^1 7s_{1/2}^2$  configurations.

### III. RESULTS AND DISCUSSION

Calculated internal conversion coefficients are presented in Table I. We estimated the half-life of the  $^{229m}\text{Th}$  isomer in the anion for the two sets of reduced nuclear probabilities given in Table II. The first set (see in Ref. [63]) was obtained with Alaga rules from the available experimental data [64–67] for the  $M1$  and  $E2$  transitions between the rotation bands  $3/2^+[631]$  and  $5/2^+[633]$  in the  $^{229}\text{Th}$  nucleus [31, 63]). The second set (taken from Ref. [68]) is based on a detailed computer calculation using modern concepts of nuclear interactions. The corresponding probabilities of radiative transitions in the  $^{229}\text{Th}$  nucleus from the isomeric to the ground state are also given in Table II.

With data presented in Tables I and II we calculate the half-life  $T_{1/2}$  of the isomer  $^{229m}\text{Th}$  in the atom and anion. The results are summarized in Table III. They must be treated with some caution. The accuracy of calculating the IIC is relatively small for the nuclear transitions with ultralow energies (see below in Table IV). This is mainly due to the accuracy of the calculation of the wave functions of valence states and their binding energies. That is why we have calculated the internal conversion probabilities not only for the thorium anion, but also for the thorium atom. Since the calculations have been performed in a unified approach, we consider these results as reliable

Table I: Internal conversion coefficients per one electron for nuclear transition with the energy  $\omega_N = 8.27$  eV for the Thorium atom in the  $6d_{3/2}^2 7s_{1/2}^2$  ground state (Th), for the Thorium anion in the  $6d_{3/2}^3 7s_{1/2}^2$  ground state ( $\text{Th}^-$ ) and in the  $6d_{3/2}^2 7s_{1/2}^2 7p_{1/2}^1$  excited state ( $\text{Th}^{-*}$ ). (The binding energies on the shells are given in parentheses).

Th	$7s_{1/2}(-6.49$ eV)	$6d_{3/2}(-7.25$ eV)	
$\alpha_{M1}$	$7.93 \times 10^8$	$2.31 \times 10^6$	
$\alpha_{E2}$	$1.06 \times 10^{15}$	$4.80 \times 10^{15}$	
$\text{Th}^-$	$7s_{1/2}(-1.60$ eV)	$6d_{3/2}(-0.63$ eV)	
$\alpha_{M1}$	$5.40 \times 10^8$	$1.45 \times 10^6$	
$\alpha_{E2}$	$6.59 \times 10^{14}$	$3.08 \times 10^{15}$	
$\text{Th}^{-*}$	$7s_{1/2}(-2.65$ eV)	$6d_{3/2}(-2.81$ eV)	$7p_{1/2}(-0.61$ eV)
$\alpha_{M1}$	$6.76 \times 10^8$	$1.21 \times 10^6$	$3.37 \times 10^7$
$\alpha_{E2}$	$6.85 \times 10^{14}$	$2.76 \times 10^{15}$	$5.44 \times 10^{16}$

Table II: Reduced matrix elements ( $B_{\text{W.u.}}$ ) of the  $3/2^+[631](8.27$  eV)  $\rightarrow$   $5/2^+[633](0.0)$  nuclear transition in the  $^{229}\text{Th}$  nucleus and corresponding radiation widths ( $\Gamma^{\text{rad}}$ ).

Set	Mult.	$B_{\text{W.u.}}$	$\Gamma^{\text{rad}}$ (eV)
1	$M1$	$3.1 \times 10^{-2}$	$3.65 \times 10^{-19}$
	$E2$	11.7	$3.06 \times 10^{-29}$
2	$M1$	$0.76 \times 10^{-2}$	$8.94 \times 10^{-20}$
	$E2$	27	$7.05 \times 10^{-29}$

for the description of relative changes in the conversion probabilities and half-lives of  $^{229m}\text{Th}$  in going from atom to anion.

As can be seen from Table III, the lifetime of the isomer in the  $6d_{3/2}^3 7s_{1/2}^2$  ground state of the anion is approximately 1.4–1.5 times longer than the isomer lifetime in the atom. For the Thorium anion in the  $6d_{3/2}^2 7s_{1/2}^2 7p_{1/2}^1$  excited state this excess is insignificant, only  $\approx 10\%$ .

This result at first glance looks counterintuitive. First, the internal conversion proceeds on four valence electrons in the thorium atom, and on five valence electrons in the anion. Second – less obvious – reason is that the electron matrix elements in the anion are larger than in the Th atom (see in Fig. 4). (Note that the latter effect is non-trivial, since, as we have seen, the WF amplitudes of the bound  $6d_{3/2}$  and  $7s_{1/2}$  states decrease upon transition

Table III:  $^{229m}\text{Th}$  isomer half life (in s) in the Th atom and in the Thorium anion in the ground ( $\text{Th}^-$ ) and in the excited ( $\text{Th}^{-*}$ ) states.

Set		Th	$\text{Th}^-$	$\text{Th}^{-*}$
1	$T_{1/2}$	$7.86 \times 10^{-7}$	$1.15 \times 10^{-6}$	$8.98 \times 10^{-7}$
	$T_{1/2}/T_{1/2}^{\text{Th}}$	1	1.47	1.14
2	$T_{1/2}$	$3.19 \times 10^{-6}$	$4.67 \times 10^{-6}$	$3.55 \times 10^{-6}$
	$T_{1/2}/T_{1/2}^{\text{Th}}$	1	1.47	1.11

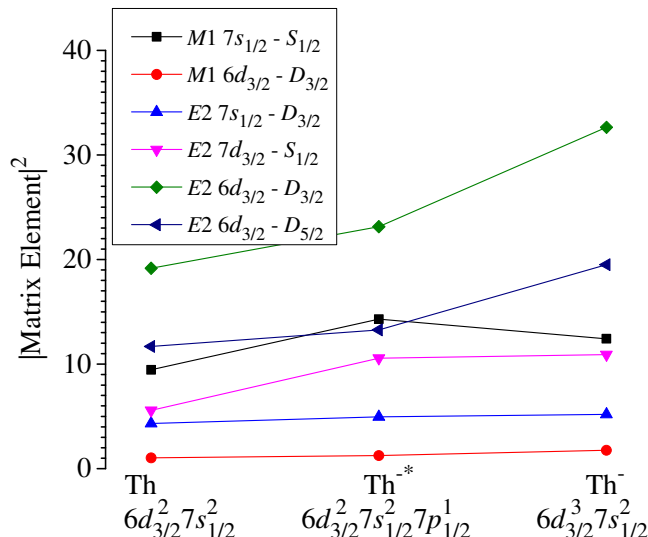


Figure 4: Matrix Elements Eq. (5) for the main IC transitions. (Matrix elements for the  $M1\ 6d_{3/2} - D_{3/2}$  electronic transitions are given in the units of  $10^{-1}$ .)

from the Th atom to the thorium anion. The matrix elements growth in Fig. 4 is explained by a faster increase in the amplitudes of the electron wave functions in the continuous spectrum with an increase of its energy (see in Fig. 3). Due to diffusion of the electron shell, the binding energies of the electrons in the Thorium anion are smaller than in the atom, and the kinetic energy of the conversion electrons in the continuum is greater. In the nonrelativistic case, the amplitudes of the Coulomb wave functions (see in [59]) in the continuum increase with the energy of the conversion electron as  $E_c^{1/4}$ , i.e. significantly faster than the decrease of the amplitudes of the wave functions in the discrete spectrum. This explains somewhat unexpected form of the plots in Fig. 4.)

There is also a third factor that places an important role in the process. This is the kinetic energy of the conversion electron in the denominator in Eq. (4). It gives the factor  $1/v$  in the expression for the IC probability and increases it near the threshold of the Th atom. In the thorium anion, this factor is 2-3 times smaller. And such a decrease turns out to be the most significant reason, which compensates for the increase in amplitudes of the electron wave functions in the continuum, and leads to a decrease in the IC probability of the anion in both the ground and excited states.

It is necessary to emphasize one more feature of the internal conversion in the anion. According to Fig. 2,  $\langle 6d_{3/2}|x|6d_{3/2}\rangle$  is the largest in the ground state of the anion. Nevertheless, the partial internal conversion coefficients on the  $6d_{3/2}$  shell in  $\text{Th}^-$  exceed ICC in  $\text{Th}^-*$  (see Table I). This is caused by the lack of the cancellation of two effects: the  $E_c^{1/4}$  increase in the amplitudes of WF of the conversion electron in the continuum and the decrease of the factor  $1/v$  for the electron promoted

Table IV: Total IC coefficients for the  $7s_{1/2}$  and  $6d_{3/2}$  shells of the Th atom obtained by different codes for the two values of the isomeric level energy:  $E_{\text{is}} = 8.28$  eV, and 7.8 eV. (In the parentheses, there are the binding energies on the shells.)

This work	$7s_{1/2}(-6.49\text{ eV})$		$6d_{3/2}(-7.25\text{ eV})$	
	$E_{\text{is}} = 8.28\text{ eV}$	$E_{\text{is}} = 7.8\text{ eV}$	8.28 eV	7.8 eV
$\alpha_{M1}$	$1.6 \times 10^9$		$4.6 \times 10^6$	
$\alpha_{E2}$	$2.1 \times 10^{15}$		$9.6 \times 10^{15}$	
Ref. [69]	$7s_{1/2}(\text{no data})$		$6d_{3/2}(\text{no data})$	
	$E_{\text{is}} = 8.28\text{ eV}$	$E_{\text{is}} = 7.8\text{ eV}$	8.28 eV	7.8 eV
$\alpha_{M1}$		$1.1 \times 10^9$		$2.0 \times 10^6$
$\alpha_{E2}$		$4.8 \times 10^{15}$		$4.3 \times 10^{15}$
Ref. [63]	$7s_{1/2}(-5.20\text{ eV})$		$6d_{3/2}(-4.20\text{ eV})$	
	$E_{\text{is}} = 8.28\text{ eV}$	$E_{\text{is}} = 7.8\text{ eV}$	8.28 eV	7.8 eV
code[70]				
$\alpha_{M1}$	$1.6 \times 10^9$	$1.9 \times 10^9$	$4.1 \times 10^6$	$4.9 \times 10^6$
$\alpha_{E2}$	$2.1 \times 10^{15}$	$2.8 \times 10^{15}$	$9.4 \times 10^{15}$	$1.3 \times 10^{16}$
Ref. [71]	$7s_{1/2}(-5.62\text{ eV})$		$6d_{3/2}(-6.10\text{ eV})$	
	$E_{\text{is}} = 8.28\text{ eV}$	$E_{\text{is}} = 7.8\text{ eV}$	8.28 eV	7.8 eV
code[72]				
$\alpha_{M1}$	$0.96 \times 10^9$	$1.1 \times 10^9$	$2.8 \times 10^6$	$3.3 \times 10^6$
$\alpha_{E2}$	$1.2 \times 10^{15}$	$1.6 \times 10^{15}$	$6.0 \times 10^{15}$	$8.0 \times 10^{15}$

during IC from the  $6d_{3/2}$  shell of  $\text{Th}^-$ . We recall that we use the energies for the bound states of the electron orbitals from Ref. [56], where the multi-configuration electron terms were taken into account. In this case, the binding energies of the terms shift up or down, while the radial wave function remains the same. As a result, one gets the indicated inconsistency between the amplitude of the radial wave function and the binding energy of the orbital. Note that this effect practically does not affect the main results of the work.

In conclusion, it will be useful to compare the total IC coefficients for the  $7s_{1/2}$  and  $6d_{3/2}$  shells of the Th atom obtained in different works and using different codes. The relevant data are given in Table IV. We see that on average all the data correspond to each other with the accuracy of the factor of two. This is sufficient for preliminary estimates of the isomer lifetime and planning of experiments. For more delicate effects, it is necessary to perform calculations within the same code.

#### IV. CONCLUSION

In the paper, for the first time, we have studied the decay of the low lying isomer  $3/2^+(8.28 \pm 0.17\text{ eV})$  of the  $^{229}\text{Th}$  nucleus in the Thorium anion. It has been found that the half life of the isomer in the  $6d_{3/2}^3 7s_{1/2}^2$  ground state of the anion is approximately 40-50% above the value in the  $6d_{3/2}^2 7s_{1/2}^2$  ground state of the Th atom and  $\approx 10\%$  larger in comparison with the  $6d_{3/2}^2 7s_{1/2}^2 7p_{1/2}^1$  excited state of the anion. The IC decay probability is correspondingly reduced, despite ‘‘extra’’ fifth electron

involved in the internal conversion process. The reason is as follows. Extra electron contributes to an additional nuclear screening for other valence electrons. As a result, the valence electron shells become more diffuse and amplitudes of the  $6d_{3/2}$  and  $7s_{1/2}$  wave functions near the

nucleus decrease. Following the amplitudes, the probability of the internal conversion decreases too.

This research was supported by a grant of the Russian Science Foundation (Project No 19-72-30014).

- 
- [1] B. Seiferle, L. von der Wense, P. V. Bilous, I. Amersdorfer, C. Lemell, F. Libisch, S. Stellmer, T. Schumm, C. E. Dullmann, A. Palfy, et al., *Nature* **573**, 243 (2019).
- [2] L. A. Kroger and C. W. Reich, *Nucl. Phys. A* **259**, 29 (1976).
- [3] C. W. Reich and R. G. Helmer, *Phys. Rev. Lett.* **64**, 271 (1990).
- [4] D. G. Burke, P. E. Garrett, T. Qu, and R. A. Naumann, *Phys. Rev. C* **42**, R499 (1990).
- [5] G. M. Irwin and K. H. Kim, *Phys. Rev. Lett.* **79**, 990 (1997).
- [6] D. S. Richardson, D. M. Benton, D. E. Evans, J. A. R. Griffith, and G. Tungate, *Phys. Rev. Lett.* **80**, 3206 (1998).
- [7] S. B. Utter, P. Beiersdorfer, A. Barnes, R. W. Lougheed, J. R. Crespo Lopez-Urrutia, J. A. Becker, and M. S. Weiss, *Phys. Rev. Lett.* **82**, 505 (1999).
- [8] E. V. Tkalya, *JETP Lett.* **70**, 371 (1999).
- [9] R. W. Shaw, J. P. Young, S. P. Cooper, and O. F. Webb, *Phys. Rev. Lett.* **82**, 1109 (1999).
- [10] E. Browne, E. B. Norman, R. D. Canaan, D. C. Glasgow, J. M. Keller, and J. P. Young, *Phys. Rev. C* **64**, 014311 (2001).
- [11] X. Zhao, Y. N. Martinez de Escobar, R. Rundberg, E. M. Bond, A. Moody, and D. J. Vieira, *Phys. Rev. Lett.* **109**, 160801 (2012).
- [12] E. Peik and K. Zimmermann, *Phys. Rev. Lett.* **111**, 018901 (2013).
- [13] R. G. Helmer and C. W. Reich, *Phys. Rev. C* **49**, 1845 (1994).
- [14] B. R. Beck, J. A. Becker, P. Beiersdorfer, G. V. Brown, K. J. Moody, J. B. Wilhelmy, F. S. Porter, C. A. Kilbourne, and R. L. Kelley, *Phys. Rev. Lett.* **98**, 142501 (2007).
- [15] L. von der Wense, B. Seiferle, M. Laatiaoui, J. B. Neumayr, H. J. Maier, H. F. Wirth, C. Mokry, J. Runke, K. Eberhardt, C. E. Dullmann, et al., *Nature* **533**, 47 (2016).
- [16] B. Seiferle, L. von der Wense, and P. G. Thirolf, *Phys. Rev. Lett.* **118**, 042501 (2017).
- [17] T. Masuda, A. Yoshimi, A. Fujieda, H. Fujimoto, H. Haba, H. Hara, T. Hiraki, H. Kaino, Y. Kasamatsu, S. Kitao, et al., *Nature* **573**, 238 (2019).
- [18] J. Thielking, M. V. Okhapkin, P. Glowacki, D. M. Meier, L. von der Wense, B. Seiferle, C. E. Dullmann, P. G. Thirolf, and E. Peik, *Nature* **556**, 321 (2018).
- [19] M. S. Safronova, S. G. Porsev, M. G. Kozlov, J. Thielking, M. V. Okhapkin, P. Glowacki, D. M. Meier, and E. Peik, *Phys. Rev. Lett.* **121**, 213001 (2018).
- [20] E. Peik and C. Tamm, *Europhys. Lett.* **61**, 181 (2000).
- [21] W. G. Rellergert, D. DeMille, R. R. Greco, M. P. Hehlen, J. R. Torgerson, and E. R. Hudson, *Phys. Rev. Lett.* **104**, 200802 (2010).
- [22] C. J. Campbell, A. G. Radnaev, A. Kuzmich, V. A. Dzuba, V. V. Flambaum, and A. Derevianko, *Phys. Rev. Lett.* **108**, 120802 (2012).
- [23] E. Peik and M. Okhapkin, *C. R. Phys.* **16**, 516 (2015).
- [24] V. V. Flambaum, *Phys. Rev. Lett.* **97**, 092502 (2006).
- [25] E. Litvinova, H. Feldmeier, J. Dobaczewski, and V. Flambaum, *Phys. Rev. C* **79**, 064303 (2009).
- [26] J. C. Berengut, V. A. Dzuba, V. V. Flambaum, and S. G. Porsev, *Phys. Rev. Lett.* **102**, 210801 (2009).
- [27] E. V. Tkalya, *Phys. Rev. Lett.* **106**, 162501 (2011).
- [28] E. V. Tkalya and L. P. Yatsenko, *Laser Phys. Lett.* **10**, 105808 (2013).
- [29] E. V. Tkalya, *Phys. Rev. Lett.* **120**, 122501 (2018).
- [30] E. V. Tkalya, *Phys. Rev. A* **94**, 012510 (2016).
- [31] A. M. Dykhne and E. V. Tkalya, *JETP Lett.* **67**, 549 (1998).
- [32] E. V. Tkalya, *Laser Phys.* **14**, 360 (2004).
- [33] E. V. Tkalya, *JETP Lett.* **71**, 311 (2000).
- [34] E. V. Tkalya, A. N. Zherikhin, and V. I. Zhudov, *Phys. Rev. C* **61**, 064308 (2000).
- [35] V. F. Strizhov and E. V. Tkalya, *Sov. Phys. JETP* **72**, 387 (1991).
- [36] P. V. Bilous, G. A. Kazakov, I. D. Moore, T. Schumm, and A. Palfy, *Phys. Rev. A* **95**, 032503 (2017).
- [37] E. V. Tkalya, *Phys. Rev. C* **100**, 054316 (2019).
- [38] Y. Shigekawa, Y. Kasamatsu, E. Watanabe, H. Ni-nomiya, S. Hayami, N. Kondo, Y. Yasuda, H. Haba, and A. Shinohara, *Phys. Rev. C* **100**, 044304 (2019).
- [39] M. Morita, *Progr. Theor. Phys.* **49**, 1574 (1973).
- [40] E. V. Tkalya, *Nucl. Phys. A* **539**, 209 (1992).
- [41] E. V. Tkalya, *Phys. Rev. A* **75**, 022509 (2007).
- [42] V. A. Krutov and V. N. Fomenko, *Ann. der Phys.* **21**, 291 (1968).
- [43] E. V. Tkalya, *JETP Lett.* **55**, 211 (1992).
- [44] E. V. Tkalya, *Sov. J. Nucl. Phys.* **55**, 1611 (1992).
- [45] P. Kalman and T. Keszthelyi, *Phys. Rev. C* **49**, 324 (1994).
- [46] E. V. Tkalya, V. O. Varlamov, V. V. Lomonosov, and S. A. Nikulin, *Phys. Scr.* **53**, 296 (1996).
- [47] S. G. Porsev, V. V. Flambaum, E. Peik, and C. Tamm, *Phys. Rev. Lett.* **105**, 182501 (2010).
- [48] S. G. Porsev and V. V. Flambaum, *Phys. Rev. A* **81**, 042516 (2010).
- [49] F. F. Karpeshin and M. B. Trzhaskovskaya, *Phys. Rev. C* **95**, 034310 (2017).
- [50] R. A. Muller, A. V. Volotka, and A. Surzhykov, *Phys. Rev. A* **99**, 042517 (2019).
- [51] P. V. Borisyuk, N. N. Kolachevsky, A. V. Taichenachev, E. V. Tkalya, I. Y. Tolstikhina, and V. I. Yudin, *Phys. Rev. C* **100**, 044306 (2019).
- [52] A. M. Dykhne, N. V. Eremin, and E. V. Tkalya, *JETP Lett.* **64**, 345 (1996).
- [53] V. O. Varlamov, A. M. Dykhne, N. V. Eremin, S. A. Nikulin, and E. V. Tkalya, *Izvestiya Akademii Nauk Seriya Fizicheskaya* **61**, 58 (1997).

- [54] E. V. Tkalya, Phys. Rev. C **60**, 054612 (1999).
- [55] S. M. Sil'nov, *Laser plasma at the late stages of expansion. Experiment, Physics, Mass Spectrometry*. (CheRo, Moscow, 2007).
- [56] R. Tang, R. Si, Z. Fei, X. Fu, Y. Lu, T. Brage, H. Liu, C. Chen, and C. Ning, Phys. Rev. Lett. **123**, 203002 (2019).
- [57] S. M. O'Malley and D. R. Beck, Phys. Rev. A **80**, 032514 (2009).
- [58] R. Si and C. F. Fischer, Phys. Rev. A **98**, 052504 (2018).
- [59] M. Abramowitz and I. A. Stegun, *Handbook of Mathematical Functions* (National Bureau of Standards, Washington, D.C., 1964).
- [60] A. Bohr and B. R. Mottelson, *Nuclear Structure. Vol. I: Single-Particle Motion*. (World Scientific, London, 1998).
- [61] A. V. Nikolaev, The FLAPW-Moscow code, Registration No. 2015616990 (Russia) from 26/06/2015.
- [62] A. V. Nikolaev, D. Lamoen, and B. Partoens, J. Chem. Phys. **145**, 014101 (2016).
- [63] E. V. Tkalya, C. Schneider, J. Jeet, and E. R. Hudson, Phys. Rev. C **92**, 054324 (2015).
- [64] C. E. Bemis, Jr., F. K. McGowan, J. L. C. Ford, Jr., W. T. Milner, R. L. Robinson, P. H. Stelson, G. A. Leander, and C. W. Reich, Phys. Scr. **38**, 657 (1988).
- [65] K. Gulda, W. Kurcewicz, A. J. Aas, M. J. G. Borge, D. G. Burked, B. Fogelberg, I. S. Grant, E. Hagebo, N. Kaffrell, J. Kvasil, et al., Nucl. Phys. A **703**, 45 (2002).
- [66] V. Barci, G. Ardisson, G. Barci-Funel, B. Weiss, O. El Samad, and R. K. Sheline, Phys. Rev. C **68**, 034329 (2003).
- [67] E. Ruchowska, W. A. Plociennik, J. Zylicz, H. Mach, J. Kvasil, A. Algora, N. Amzal, T. Back, M. G. Borge, R. Boutami, et al., Phys. Rev. C **73**, 044326 (2006).
- [68] N. Minkov and A. Palffy, Phys. Rev. Lett. **118**, 212501 (2017).
- [69] P. V. Bilous, N. Minkov, and A. Palffy, Phys. Rev. C **97**, 044320 (2018).
- [70] A. A. Soldatov and D. P. Grechukhin, Kurchatov Institute of Atomic Energy Report-3174, Moscow, 1979.
- [71] P. V. Borisyuk, U. N. Kurel'chuk, O. S. Vasil'ev, V. I. Troyan, Y. Y. Lebedinskii, and E. V. Tkalya, Quant. Electron. **48**, 460 (2018).
- [72] I. M. Band and V. I. Fomichev, At. Data Nucl. Data Tabl. **23**, 295 (1979).